ANL-7551

ANL-7551

RETURN TO ANL (IDAHO) LIBRARY.

Argonne National Laboratory

ANALYSIS OF MAGNETIC FIELDS IN A METAL

by

D. L. Waidelich

The facilities of Argonne National Laboratory are owned by the United States Government. Under the terms of a contract (W-31-109-Eng-38) between the U. S. Atomic Energy Commission, Argonne Universities Association and The University of Chicago, the University employs the staff and operates the Laboratory in accordance with policies and programs formulated, approved and reviewed by the Association.

MEMBERS OF ARGONNE UNIVERSITIES ASSOCIATION

The University of Arizona
Carnegie-Mellon University
Case Western Reserve University
The University of Chicago
University of Cincinnati
Illinois Institute of Technology
University of Illinois
Indiana University
Iowa State University
The University of Iowa
Kansas State University
The University of Kansas
Loyola University
Marquette University
Michigan State University
The University of Michigan
University of Minnesota
University of Missouri
Northwestern University
University of Notre Dame
The Ohio State University
Ohio University
The Pennsylvania State University
Purdue University
Saint Louis University
Southern Illinois University
University of Texas
Washington University
Wayne State University
The University of Wisconsin

LEGAL NOTICE

This report was prepared as an account of Government sponsored work. Neither the United States, nor the Commission, nor any person acting on behalf of the Commission:

A. Makes any warranty or representation, expressed or implied, with respect to the accuracy, completeness, or usefulness of the information contained in this report, or that the use of any information, apparatus, method, or process disclosed in this report may not infringe privately owned rights; or

B. Assumes any liabilities with respect to the use of, or for damages resulting from the use of any information, apparatus, method, or process disclosed in this report.

As used in the above, "person acting on behalf of the Commission" includes any employee or contractor of the Commission, or employee of such contractor, to the extent that such employee or contractor of the Commission, or employee of such contractor prepares, disseminates, or provides access to, any information pursuant to his employment or contract with the Commission, or his employment with such contractor.

Printed in the United States of America
Available from
Clearinghouse for Federal Scientific and Technical Information
National Bureau of Standards, U. S. Department of Commerce
Springfield, Virginia 22151
Price: Printed Copy \$3.00; Microfiche \$0.65

ANL-7551
Physics

ARGONNE NATIONAL LABORATORY
9700 South Cass Avenue
Argonne, Illinois 60439

ANALYSIS OF MAGNETIC FIELDS IN A METAL

by

D. L. Waidelich

University of Missouri, Columbia, Missouri
Visiting Scientist, ANL

Metallurgy Division
Program 12.1.13

May 1969

TABLE OF CONTENTS

LIST OF FIGURES

ANALYSIS OF MAGNETIC FIELDS IN A METAL

by

D. L. Waidelich

ABSTRACT

In the nondestructive testing of metals, experimental measurements had shown that the attenuation of electromagnetic waves originating from a masked probe and passing through a thin sheet of metal was much less than that predicted by the use of a mathematical model employing plane waves with the pulsed magnetic vector parallel to the surface of the metal. An analysis was made by assuming that the pulsed magnetic vector was perpendicular to the surface of the metal. The results of both analyses indicated that the attenuation in the metal was the same and was very nearly equal to the attenuation observed experimentally. The plane-wave analysis with the magnetic vector parallel to the metal surface, however, would require a large attenuation at the air-to-metal and the metal-to-air boundaries, whereas the analysis with the magnetic vector perpendicular to the metal surface would probably require very little attenuation at these surfaces. These findings seem to indicate that the observed difference is caused by the reflections occurring at the air-to-metal and the metal-to-air boundaries, and that the analysis with the magnetic vector perpendicular to the surface of the metal will predict very nearly the attenuation observed experimentally.

I. INTRODUCTION

Masked probes have proven to be a useful addition to pulsed eddy-current techniques for nondestructive testing.[1] An analysis of the pulsed electromagnetic fields and currents near the probe is needed to aid in the design of the probes[2] since previous analyses[3,4] with plane waves gave very low values for the field transmitted through a metal sheet as compared with values measured experimentally.[5,6] A first attempt[7,8] to provide the necessary analysis assumed a horizontal magnetic field above a plane metal surface with the field appearing as a step function in time. Since the driving field from a masked probe has, for the most part, a vertical component, a vertical magnetic field was used rather than a horizontal field. A unit impulse in time was used as the driving function so that the results would be

simpler to interpret than the results for a unit step function. The use of a convolution integral will enable the results for any driving function to be obtained. A two-dimensional analysis was used for simplicity.

II. THEORY

By using the Maxwell equations as given in Appendix A, the following expressions result for the magnetic and electric fields in a conductor:

$$\hat{\bar{H}} = (\sigma + \epsilon s) \nabla \times \hat{\bar{\pi}} \tag{1}$$

and

$$\hat{\bar{E}} = \nabla(\nabla \times \hat{\bar{\pi}}) - \mu s(\sigma + \epsilon s) \hat{\bar{\pi}}, \tag{2}$$

where the Laplace transform $\hat{\bar{\pi}}$ of vector potential $\bar{\pi}$ is found from the wave equation

$$\nabla^2 \hat{\bar{\pi}} - \mu s(\sigma + \epsilon s) \hat{\bar{\pi}} = 0, \tag{3}$$

and σ = conductivity of the conductor, ϵ = permittivity of the conductor, μ = permeability of the conductor, and s = complex variable as used in the Laplace transform.

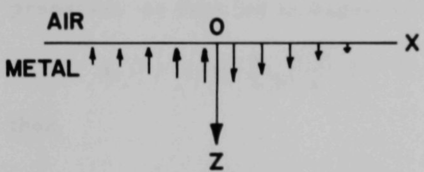

306-341 Rev. 1

Fig. 1. Assumed Variation of the Magnetic Field at the Surface of the Metal

A two-dimensional geometry was used for simplicity, and the metal was assumed to be semi-infinite in extent, as shown in Fig. 1. The following assumptions were made:

(1) The y axis extends out from the paper, and there is no variation with y.

(2) The xy plane is the surface of the metal. The vertical magnetic field in the surface of the metal is an odd function of x (as shown in Fig. 1) and varies as $e^{-(x/x_0)}$, where x_0 is a constant that represents the distance from the origin in which the field intensity decreases to e^{-1}.

(3) The applied vertical magnetic field varies as unit impulse in time.

The vector potential then could have a component $\hat{\pi}$ in the y direction only. In addition, if the displacement current in the metal is assumed very small compared with the conduction current, Eq. (3) becomes

$$\frac{\partial^2 \hat{\pi}}{\partial x^2} + \frac{\partial^2 \hat{\pi}}{\partial z^2} - \sigma\mu s \hat{\pi} = 0. \tag{4}$$

Differential Eq. (4) was solved and the boundary conditions applied as indicated in Appendix B. In the metal, the vertical magnetic field obtained from the vector potential is

$$H_z = \frac{V e^{-V^2} e^{W^2}}{2\pi^{1/2} t} \left[e^{-2uW} \operatorname{Erfc}(W - u) - e^{2uW} \operatorname{Erfc}(W + u) \right], \tag{5}$$

where

$$u = \frac{x}{2}\sqrt{\frac{\sigma\mu}{t}}; \quad V = \frac{z}{2}\sqrt{\frac{\sigma\mu}{t}}; \quad W = \frac{1}{x_0}\sqrt{\frac{t}{\sigma\mu}}.$$

Equation (5) represents the vertical magnetic field anywhere in the metal for a unit impulse of vertical magnetic field at the metallic surface, and for an exponential decrease of field in the x direction.

To obtain the effect of a field that is constant with distance in the x direction, the case of x_0 approaching infinity was studied. This might, for example, represent the variation of the field immediately under a masked probe with the distance x magnified considerably so that the field appears to remain constant with x, at least until x becomes quite large. An additional advantage is that two variables are eliminated from the expressions, as detailed in Appendix C. Under the conditions that

$$x_0 >> x \text{ and } \frac{x}{2}\sqrt{\frac{\sigma\mu}{t}} >> 1,$$

then

$$H_z = \frac{V e^{-V^2}}{\pi^{1/2} t} = \frac{4V^3 e^{-V^2}}{\pi^{1/2} \sigma\mu z^2}. \tag{6}$$

In Eq. (6) put

$$\frac{\pi^{1/2}\sigma\mu z^2}{4} H_z = V^3 e^{-V^2} = f(V). \tag{7}$$

A plot of f(V) versus V is shown in Fig. 2. As t increases, V decreases and, from Fig. 2, the vertical magnetic field starts at zero, increases to a maximum, and then decreases to zero again.

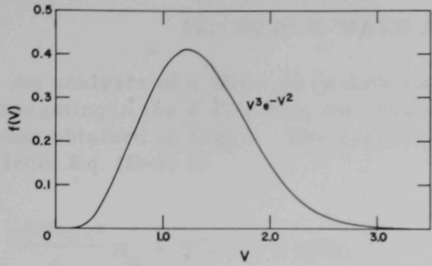

Fig. 2
Variation of the Vertical Magnetic Field in the Metal

306-342

III. EXPERIMENTAL AGREEMENT

To verify Eq. (6), the curve of magnetic field intensity with no metal present was used as the driving field. This curve was divided into six parts, each 0.5 μs long, and each part was regarded as a separate magnetic impulse. We assumed that each impulse was applied to a 5/64-in. plate of Type 304 stainless steel with the conductivity of $\sigma = 1.39 \times 10^6$ mho/m and the relative permeability of 1.02. A convolution integral was evaluated numerically by using the above impulses along with Fig. 2, and the result is shown as the calculated curve in Fig. 3. The measured curve of Fig. 3 (from Fig. 5 of Ref. 11) is the magnetic intensity after the field passed through the stainless steel plate. The magnitudes of the measured and calculated peaks of Fig. 3 are nearly the same, but the calculated peak occurs later and decreases in magnitude much more slowly than the measured peak. The applied pulse probably had a negative tail, which was not shown since conduction in the thyratron used to obtain the pulse would continue until the thyratron was completely deionized. The effect of the negative tail would move the calculated peak to the left and make the calculated curve drop much faster than that shown after the peak had been passed; the peak also would be reduced slightly.

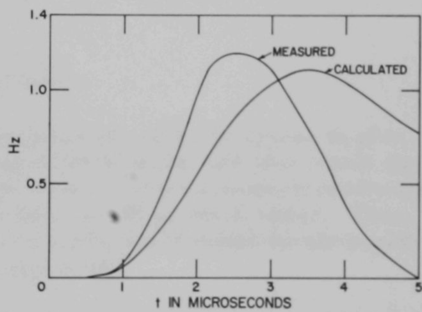

306-343

Fig. 3. Calculated and Measured Curves of the Vertical Magnetic Field after Passing through a Stainless Steel Sheet

Note also that this analysis is for two dimensions, whereas the measurements were made in a three-dimensional setup. The effects of the air-to-metal and metal-to-air surfaces were disregarded. Another important assumption is that, from Eq. (6), the field in the metal resembles the field from a solenoidal-type probe placed in the air immediately above the metal.

Variation of the Vertical Magnetic Field in the Metal

306-382

III. EXPERIMENTAL AGREEMENT

To verify Eq. (6), the curve of magnetic field intensity with no metal present was used as the driving field. This curve was divided into six parts, each 0.5 μs long, and each part was regarded as a separate magnetic impulse. We assumed that each impulse was applied to a 5/64-in. plate of Type 304 stainless steel with the conductivity of $\sigma = 1.39 \times 10^6$ mho/m and the relative permeability of 1.02. A convolution integral was evaluated numerically by using the above impulses along with Fig. 2, and the result is shown as the calculated curve in Fig. 3. The measured curve of Fig. 3 (from Fig. 5 of Ref. 11) is the magnetic intensity after the field passed through the stainless steel plate. The magnitudes of the measured and calculated peaks of Fig. 3 are nearly the same, but the calculated peak occurs later and decreases in magnitude much more slowly than the measured peak. The applied pulse probably had a negative tail, which was not shown since conduction in the thyratron used to obtain the pulse would continue until the thyratron was completely deionized. The effect of the negative tail would move the calculated peak to the left and make the calculated curve drop much faster than that shown after the peak had been passed; the peak also would be reduced slightly.

306-348

Fig. 3. Calculated and Measured Curves of the Vertical Magnetic Field after Passing through a Stainless Steel Sheet

Note also that this analysis is for two dimensions, whereas the measurements were made in a three-dimensional setup.* The effects of the air-to-metal and metal-to-air surfaces were disregarded. Another important assumption is that, from Eq. (6), the field in the metal resembles the field from a solenoidal-type probe placed in the air immediately above the metal.

IV. PLANE-WAVE ANALYSIS

An analysis of a plane wave with fields parallel to the metal surface and propagating in the z direction was expected to give far different results than those obtained in Fig. 3. The analysis is presented in Appendix D; the result from Eq. (D-6) is

$$\frac{\pi^{1/2}\sigma\mu z^2}{4} H_x = V^3 e^{-V^2} = f(V), \qquad (8)$$

which is exactly Eq. (7) except that H_z has been replaced by H_x. Then, if the magnetic plane-wave pulse in the metal is of the form of Fig. 5 of Ref. 11, the resulting calculated horizontal magnetic field must be that of Fig. 3. Hence, either type of field would appear to give the same response in going through a stainless steel plate, except for the direction of the field. A receiving coil was placed so that it would receive a vertical field much better than a horizontal field. Since experiments seem to indicate a much larger response for a vertical field compared with the calculated horizontal plane-wave type of response, the difference is probably in the air-to-metal and metal-to-air boundaries.

V. CONCLUSIONS

The vertical and horizontal plane-wave calculations appear to give the same result for transmission through a metal plate, and this result appears to agree fairly well with measured values. If the boundary conditions are considered, the result for the plane wave would be much lower. Thus, further studies should be made of the air-to-metal and metal-to-air boundary conditions when a vertical wave is impressed.

Other problems that should be investigated are a space-impulse configuration of applied field and three-dimensional studies rather than the two-dimensional work in this report. The space-impulse configuration would probably approach that of an aperture in a mask fairly closely.

APPENDIX A

Vector Potential

In a conductor, the Laplace transform of the Maxwell equations for the magnetic field intensity $\overline{H}$ and electric field intensity $\overline{E}$ are

$$\nabla \times \hat{\overline{E}} = -\mu s \hat{\overline{H}}, \qquad \text{(A-1)}$$

where μ is the permeability of the conductor, and s is the complex variable for the Laplace transform; further

$$\nabla \times \hat{\overline{H}} = (\sigma + \epsilon s)\, \hat{\overline{E}}, \qquad \text{(A-2)}$$

where σ is the conductivity, and ϵ is the permittivity of the conductor. Let

$$\hat{\overline{H}} = (\sigma + \epsilon s)\, \nabla \times \hat{\overline{\pi}}, \qquad \text{(A-3)}$$

where $\hat{\overline{\pi}}$ is the vector potential.

Substitute Eq. (A-3) in Eq. (A-1) to get

$$\nabla \times \left[\hat{\overline{E}} + \mu s(\sigma + \epsilon s)\, \hat{\overline{\pi}}\right] = 0, \qquad \text{(A-4)}$$

or

$$\hat{\overline{E}} = -\mu s(\sigma + \epsilon s)\, \hat{\overline{\pi}} - \nabla \hat{\Phi},$$

where $\hat{\Phi}$ is the transform of a scalar function Φ. Now, by substituting Eq. (A-3) in Eq. (A-2),

$$\hat{\overline{E}} = \nabla \times \nabla \times \hat{\overline{\pi}} = \nabla\left(\nabla \cdot \hat{\overline{\pi}}\right) - \nabla^2 \hat{\overline{\pi}}. \qquad \text{(A-5)}$$

Use the gauge

$$\nabla \cdot \hat{\overline{\pi}} = -\hat{\Phi} \qquad \text{(A-6)}$$

and substitute Eq. (A-6) into Eqs. (A-4) and (A-5) to obtain

$$\nabla^2 \hat{\overline{\pi}} - \mu s(\sigma + \epsilon s)\, \hat{\overline{\pi}} = 0. \qquad \text{(A-7)}$$

From Eqs. (A-5) and (A-7),

$$\hat{\overline{E}} = \nabla\left(\nabla \cdot \hat{\overline{\pi}}\right) - \mu s\, (\sigma + \epsilon s)\, \hat{\overline{\pi}}. \qquad \text{(A-8)}$$

If differential Eq. (A-7) is solved for $\hat{\overline{\pi}}$, the magnetic and electric field intensities may be determined from Eqs. (A-3) and (A-8).

APPENDIX B

Derivation of Fields

Assuming that the vector potential has only a y component $\hat{\pi}$ and that the displacement current in the metal may be neglected, then

$$\frac{\partial^2 \hat{\pi}}{\partial x^2} + \frac{\partial^2 \hat{\pi}}{\partial z^2} = \sigma \mu s \hat{\pi}. \tag{B-1}$$

The solution of Eq. (B-1) is

$$\hat{\pi} = \int_0^\infty A(\alpha) e^{-\gamma z} (\cos \alpha x)\, d\alpha, \tag{B-2}$$

where α is the eigenvalue, $A(\alpha)$ is a function to be determined from the boundary conditions, and

$$\gamma = \sqrt{\sigma \mu s + \alpha^2}. \tag{B-3}$$

From $\hat{\hat{H}} = \sigma \nabla \times \hat{\hat{\pi}}$,

$$\hat{H}_x = -\sigma \frac{\partial \hat{\pi}}{\partial z} = \sigma \int_0^\infty \gamma A(\alpha) e^{-\gamma z} (\cos \alpha x)\, d\alpha, \tag{B-4}$$

and

$$\hat{H}_z = \sigma \frac{\partial \hat{\pi}}{\partial x} = -\sigma \int_0^\infty \alpha A(\alpha) e^{-\gamma z} (\sin \alpha x)\, d\alpha. \tag{B-5}$$

From $\hat{\hat{E}} = \nabla(\nabla \cdot \hat{\hat{\pi}}) - \sigma \mu s \hat{\hat{\pi}}$,

$$\hat{E}_y = -\sigma \mu s \int_0^\infty A(\alpha) e^{-\gamma z} (\cos \alpha x)\, d\alpha. \tag{B-6}$$

The other field components $\hat{H}_y$, $\hat{E}_x$, and $\hat{E}_z$ are all zero.

At the surface of the metal

$$\hat{H}_z \Big|_{z=0} = e^{-(x/x_0)} = -\sigma \int_0^\infty \alpha A(\alpha) (\sin \alpha x)\, d\alpha. \tag{B-7}$$

When the inverse Fourier transform of Eq. (B-7) is used

$$A(\alpha) = -\frac{2}{\pi\sigma\left(\alpha^2 + \frac{1}{x_0^2}\right)}. \tag{B-8}$$

From Eqs. (B-2) and (B-8),

$$\hat{\pi} = -\frac{2}{\pi\sigma}\int_0^\infty \frac{e^{-z\sqrt{\sigma\mu s + \alpha^2}}}{\left(\alpha^2 + \frac{1}{x_0^2}\right)}(\cos\alpha x)\,d\alpha. \tag{B-9}$$

From Eq. (14), p. 246 of Ref. 9 and by use of the shifting theorem,

$$L^{-1}\left(e^{-z\sqrt{\sigma\mu s + \alpha^2}}\right) = \frac{z\sqrt{\sigma\mu}\,e^{-(\alpha^2 t/\sigma\mu)}e^{-(\sigma\mu z^2/4t)}}{2\pi^{1/2}t^{3/2}}. \tag{B-10}$$

When Eq. (B-10) is placed in the inverse Laplace transform of Eq. (B-9),

$$\pi_y = -\frac{z\sqrt{\mu/\sigma}}{(\pi t)^{3/2}}\,e^{-(\sigma\mu z^2/4t)}\int_0^\infty \frac{e^{-(\alpha^2 t/\sigma\mu)}\,(\cos\alpha x)}{\left(\alpha^2 + \frac{1}{x_0^2}\right)}\,dx, \tag{B-11}$$

where $\pi_y = L^{-1}(\hat{\pi})$.

From Eq. (15), p. 15 of Ref. 10,

$$\pi_y = -\frac{x_0 z\sqrt{\mu/\sigma}}{4\pi^{1/2}t^{3/2}}\,e^{-(\sigma\mu z^2/4t)}e^{(t/\sigma\mu x_0^2)}$$

$$\left[e^{-(x/x_0)}\,\mathrm{Erfc}\left(\frac{1}{x_0}\sqrt{\frac{t}{\sigma\mu}} - \frac{x}{2}\sqrt{\frac{\sigma\mu}{t}}\right) + e^{(x/x_0)}\,\mathrm{Erfc}\left(\frac{1}{x_0}\sqrt{\frac{t}{\sigma\mu}} + \frac{x}{2}\sqrt{\frac{\sigma\mu}{t}}\right)\right]. \tag{B-12}$$

Let

$$u = \frac{x}{2}\sqrt{\frac{\sigma\mu}{t}}; \quad V = \frac{z}{2}\sqrt{\frac{\sigma\mu}{t}}; \quad W = \frac{1}{x_0}\sqrt{\frac{t}{\sigma\mu}}; \tag{B-13}$$

then Eq. (B-12) becomes

$$\pi_y = -\frac{Ve^{-V^2}e^{W^2}}{2\pi^{1/2}\sigma\sqrt{\sigma\mu}t^{1/2}W}\left[e^{-2uW}\,\mathrm{Erfc}(W-u) + e^{2uW}\,\mathrm{Erfc}(W+u)\right]. \tag{B-14}$$

From Eqs. (B-4), (B-5), (B-6), and (B-14),

$$H_z = \frac{Ve^{-V^2}e^{W^2}}{2\pi^{1/2}t}\left[e^{-2uW}\,\mathrm{Erfc}(W-u) - e^{2uW}\,\mathrm{Erfc}(W+u)\right], \tag{B-15}$$

$$H_x = \frac{(1-2V^2)\,e^{-V^2}e^{W^2}}{4\pi^{1/2}tW}\left[e^{-2uW}\,\mathrm{Erfc}(W-u) + e^{2uW}\,\mathrm{Erfc}(W+u)\right], \tag{B-16}$$

and

$$E_y = \frac{\sqrt{\mu/\sigma}\;Ve^{-V^2}e^{W^2}\left(V^2+W^2-3/2\right)}{2\pi^{1/2}t^{3/2}W}\left[e^{-2uW}\,\mathrm{Erfc}(W-u) + e^{2uW}\,\mathrm{Erfc}(W+u)\right]. \tag{B-17}$$

The current density i_y is

$$i_y = \sigma E_y. \tag{B-18}$$

The quantities u, V, and W are dimensionless, and since the applied field is a unit impulse or 1 A-sec/m, the dimension of the magnetic field intensity should be the unit impulse divided by time. This can be verified by noting the units of H_z in Eq. (B-15) and those of H_x in Eq. (B-16).

APPENDIX C

The Constant-field Case

As x_0 approaches infinity ($W \rightarrow 0$) the applied vertical magnetic field approaches a constant with distance, except for the reversal of the field direction for negative values of x as compared with positive values of x. The potential π_y also approaches infinity in magnitude, but the vertical magnetic field from Eq. (B-15) approaches

$$H_z = \frac{Ve^{-V^2}}{\pi^{1/2}t} \text{ Erfu.} \tag{C-1}$$

The other field components also approach infinity.

If x_0 is taken as very large but finite, Eq. (C-1) may be used as a good approximation to the vertical field in the metal. More exactly, to use Eq. (C-1), $2uW \ll 1$, $W << u$ or $(x/x_0) \ll 1$, and $(xx_0/2)(\sigma\mu/t) >> 1$. In addition, if $u \gg 1$ [i.e., $(x/2)\sqrt{\sigma\mu/t} >> 1$], then Eq. (C-1) may be replaced by

$$H_z = \frac{Ve^{-V^2}}{\pi^{1/2}t}. \tag{C-2}$$

To use Eq. (C-2), the above three inequalities may then be replaced by the two inequalities $x_0 \gg x$ and $(x/2)\sqrt{\sigma\mu/t} >> 1$.

APPENDIX D

Plane-wave Analysis

The assumed configuration was again that of Fig. 1 except that now both the electric and magnetic fields were parallel to the surface of the metal. Since the only variation present would be inthe z direction, Eq. (3) becomes

$$\frac{d^2\hat{\pi}}{dz^2} = \sigma\mu s\hat{\pi}, \tag{D-1}$$

where $\hat{\pi}$ is the vector potential in the y direction. Then

$$\hat{\pi} = Ae^{-z\sqrt{\sigma\mu s}}, \tag{D-2}$$

where A is a constant. From Eq. (1),

$$\hat{H}_x = -\sigma\frac{d\hat{\pi}}{dz} = \sigma\sqrt{\sigma\mu s}\,Ae^{-z\sqrt{\sigma\mu s}}. \tag{D-3}$$

Assume that H_x at the surface of the metal is a unit impulse, and that

$$\hat{H}_x\Big|_{z=0} = 1 = \sigma\sqrt{\sigma\mu s}\,A \text{ or } A = \frac{1}{\sigma\sqrt{\sigma\mu s}}. \tag{D-4}$$

Substitute Eq. (D-4) in Eq. (D-2) and take the inverse Laplace transform to get

$$\pi_y = \frac{e^{-(\sigma\mu z^2/4t)}}{\sigma\sqrt{\sigma\mu\pi t}}. \tag{D-5}$$

Then,

$$H_x = -\sigma\frac{\partial\pi_y}{\partial z} = \frac{4V^3e^{-V^2}}{\pi^{1/2}\sigma\mu z^2} \text{ or } \frac{\pi^{1/2}\sigma\mu z^2}{4}H_x = V^3e^{-V^2} = f(V). \tag{D-6}$$

REFERENCES

1. C. J. Renken, *A Pulsed Eddy Current Test System Using Reflected Fields*, Mat. Eval. *23*, 622-627 (Dec 1965).

2. C. J. Renken, *A Pulsed Electromagnetic Test System Applied to the Inspection of Thin-walled Tubing*, ANL-6728 (March 1964).

3. L. M. Vallese, *Diffusion of Pulsed Currents in Conductors*, J. Appl. Phys. *25*, 225-228 (Feb 1954).

4. D. L. Waidelich, J. A. DeShong, and W. J. McGonnagle, *A Pulsed Eddy Current Technique for Measuring Clad Thickness*, ANL-5614 (July 1958).

5. C. J. Renken, *Suppression and Reduction of Noise in Electromagnetic Test Systems*, ANL-7155 (1965).

6. C. W. Cox and C. J. Renken, *The Use of the Conducting Mask in Pulsed Electromagnetic Testing*, ANL-7172 (in press).

7. D. L. Waidelich, *Analysis of Pulsed Electromagnetic Probes*, University of Missouri Final Report on Contract 31-109-38-1873 with Argonne National Laboratory, Jan. 31, 1967.

8. D. L. Waidelich, *An Analysis of the Pulsed Magnetic Field Under a Masked Eddy-Current Probe*, Proceedings of the Fourth Congress on Materials Testing, Budapest, Hungary, Oct. 11-14, 1967, Vol. 3, pp. 879-892.

9. G. E. Roberts and H. Kaufman, *Table of Laplace Transforms*, W. B. Saunders Co. (1966).

10. A. Erdelyi, *Tables of Integral Transforms*, Vol. I, McGraw-Hill Book Co., Inc., New York (1954).

11. C. J. Renken, *The Diffusion of Pulsed Current Fields in Good Conductors*, ANL-6346, pp. 127-138 (Oct 1960).

ARGONNE NATIONAL LAB WEST
3 4444 00007941 8